Soft Dropping Power Control

Roy D. Yates, Sorabh Gupta, Christopher Rose, Surgwon Sohn
Wireless Information Network Laboratory
ryates@winlab.rutgers.edu, sorabhg@winlab.rutgers.edu, crose@winlab.rutgers.edu, ssogn@ece.rutgers.edu
Rutgers, The State University of New Jersey, P.O. Box 909, Piscataway, New Jersey 08855-0909

***Abstract*— This work considers a power control algorithm for cellular communications systems in which a user's link quality objective, as measured by signal to interference ratio (SIR), varies with its transmitter power. In particular, as increased interference or reduced uplink gain leads a mobile to raise its transmitter power, that mobile lowers its SIR target. In this way, the likelihood of an infeasible power control problem in which users' transmitter powers rise to maximum is reduced. This graceful degradation of the SIR is termed soft dropping. Convergence proofs for a soft dropping power control algorithm are outlined. Simulation results demonstrate performance improvements over fixed target SIR algorithms.**

I. Introduction

In power control for cellular communications, analytical methods have derived convergence results for iterative power control algorithms that meet SIR requirements. [1]–[12] On occasion, it is not possible for every user to meet its SIR target. In this case when the power control problem is infeasible, transmitter powers will diverge or, in the presence of maximum power constraints, some users will reach maximum transmitter power without achieving the target SIR [11]–[14]. This can result in dropped connections or additional handoffs to neighboring base stations.

In this work, target SIR is not a fixed value, but a variable one that ranges from maximum $\bar{\Gamma}$ to minimum $\hat{\Gamma}$. In particular, as a mobile raises its transmitted power, in response to either increased interference or reduced uplink gain, that mobile will lower its SIR target. That is, as we would normally approach an infeasible power control problem in which transmitter powers rapidly escalate, the variable target SIR algorithm encourages a user to aim for a lower SIR target to increase the likelihood that all users can be supported. Since a user's target SIR gradually decreases as its transmitter power rises, we call this approach *soft dropping*.

The use of variable SIR targets has been studied by simulation in [15] where it is found that the approach can yield significant performance improvements. In this work, a convergence proof for a soft dropping power control algorithm that enforces both minimum and maximum transmitter power constraints will be given. In addition, simulation studies of soft dropping will be presented for a system similar to GSM.

II. Soft Dropping Interference Constraints

We will consider the uplink of a cellular communication system of n users in which signals of other users can be modeled as interfering signals. Let p_j denote the transmitter power of user j, and h_{kj} denote the propagation gain of user j to base k. At base k, the received signal power from user j is $h_{kj}p_j$ while the interference is $\sum_{i\neq j} h_{ki}p_i + N_0$ where N_0 denotes the receiver noise power at base k. Hence under power vector $\boldsymbol{p} = [p_1, \cdots, p_n]$, the SIR of user j at its assigned base station a_j can be written as

$$\gamma_j(\boldsymbol{p}) = \frac{p_j}{I_j(\boldsymbol{p})} \tag{1}$$

where

$$I_j(\boldsymbol{p}) = \frac{\sum_{i\neq j} h_{a_j i}p_i + N_0}{h_{a_j j}} \tag{2}$$

Although we describe the users' link SIRs in the context of a fixed assignment of users to base stations, we will see that the soft dropping approach is applicable whenever each user's SIR can be expressed in the form of (1) for a standard interference function $\boldsymbol{I}(\boldsymbol{p}) = [I_1(\boldsymbol{p}), \cdots, I_n(\boldsymbol{p})]$; see [12].

In a fixed target power control algorithm, each user iteratively adjusts its power in order to find a power vector $\boldsymbol{p}$ such that for every user j, $\gamma_j(\boldsymbol{p}) \geq \Gamma_j$. In the soft dropping power control algorithm, the SIR requirement of user j must satisfy

$$\gamma_j(\boldsymbol{p}) \geq \Gamma_j(p_j) \tag{3}$$

In this case, $\Gamma_j(p_j)$, the target SIR of user j, is varied according to the user's transmitter power p_j as depicted in Figure 1. Note that at all times, each user j aims for a target SIR that is above a dropping threshold $\Gamma_j^{(d)}$ For $p_j \leq \bar{q}_j$, user j attempts to maintain a high quality connection by aiming for a target SIR $\overline{\Gamma}_j$. For $\hat{q}_j \leq p_j \leq p_j^{\max}$, user j aims for an acceptable target SIR $\hat{\Gamma}_j$. Note that $\overline{\Gamma}_j \geq \hat{\Gamma}_j \geq \Gamma_d$. For

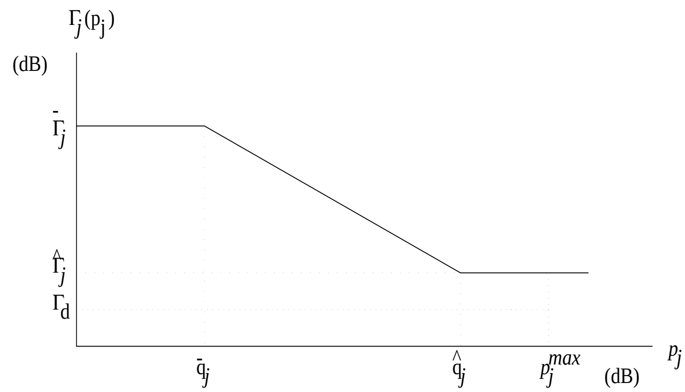

Fig. 1. The variable SIR target $\Gamma_j(p_j)$

$\bar{q}_j < p_j < \hat{q}_j$, user j aims for a target SIR $\Gamma_j^{(v)}(p_j)$ that trades SIR for transmitter power linearly in dB.

In [6], [7], it is observed that a fixed SIR target iterative algorithm can be written as

$$p_j(t+1) = \left(\frac{\Gamma_j}{\gamma_j(\boldsymbol{p}(t))}\right)^{\beta_j} p_j(t) \tag{4}$$

where β_j is an arbitrary constant satisfying $0 < \beta_j \le 1$. That is, when user j has SIR $\gamma_j(\boldsymbol{p})$ that is less than Γ_j, user j raises its transmitter power. Conversely, when the SIR of user j is above the target Γ_j, user j lowers its power. The effect of the exponent β_j can be seen by expressing the power control iteration in logarithmic terms. From (4), we can write

$$\log p_j(t+1) = (1-\beta_j)\log p_j(t) + \beta_j \log\left(\Gamma_j I_j(\boldsymbol{p}(t))\right) \tag{5}$$

For $0 < \beta_j < 1$, we see that in dB, user j chooses a weighted average of its current transmitter power $p_j(t)$ and the necessary power $\Gamma_j I_j(\boldsymbol{p}(t))$ for SIR Γ_j. Typically, we will see in simulations that small β_j results in slow convergence of the power control algorithm.

Similar to (4), a variable SIR target iteration can be expressed as

$$\boldsymbol{p}_j(t+1) = \boldsymbol{T}(\boldsymbol{p}_j(t)) = \left(\frac{\Gamma_j(p_j)}{\gamma_j(\boldsymbol{p})}\right)^{\beta_j} p_j \tag{6}$$

At this point, it is not clear that the iteration (6) will converge. In particular, it is easy to imagine oscillatory effects in which user j has low transmitted power and aims for high SIR, leading user j to have high power and aim for low SIR resulting in low transmitter power. As we shall see, convergence results for the iteration (6) will depend on the careful choice of the β_j.

Finally, it will be desirable to consider minimum and maximum power limits $\boldsymbol{p}^{\min}$ and $\boldsymbol{p}^{\max}$. We define the constrained iteration $\boldsymbol{T}^*(\boldsymbol{p})$ by

$$\boldsymbol{T}_j^*(\boldsymbol{p}) = \max\left\{p_j^{\min}, \min\left\{p_j^{\max}, T_j(\boldsymbol{p})\right\}\right\} \tag{7}$$

In this case, $\boldsymbol{p}^{\min} \le \boldsymbol{T}^*(\boldsymbol{p}) \le \boldsymbol{p}^{\max}$. Whenever the iteration function $\boldsymbol{T}(p)$ would require a power over the maximum or under the minimum, the power chosen is constrained. We will show that the constrained variable SIR target power control iteration

$$\boldsymbol{p}(t+1) = \boldsymbol{T}^*(\boldsymbol{p}(t)) \tag{8}$$

will always converge to a unique fixed point at which each user's variable SIR target will be met subject to the minimum and maximum power constraints.

III. Standard Interference Functions

To verify convergence of the iteration (8), we will use the approach of [12] which analyzes power control algorithms of the form

$$\boldsymbol{p}(t+1) = \boldsymbol{I}(\boldsymbol{p}(t)) \tag{9}$$

For the uplink of a variety of single channel cellular systems, the interference function $\boldsymbol{I}(\boldsymbol{p})$ was shown to be *standard* in the following sense.

Definition 1: $\boldsymbol{I}(\boldsymbol{p})$ is a standard interference function if for all $\boldsymbol{p} \ge 0$, the following properties are satisfied.

- (Positivity) $\boldsymbol{I}(\boldsymbol{p}) > 0$
- (Monotonicity) If $\boldsymbol{p} \ge \boldsymbol{p}'$, then $\boldsymbol{I}(\boldsymbol{p}) \ge \boldsymbol{I}(\boldsymbol{p}')$
- (Scalability) For all $\alpha > 1$, $\alpha \boldsymbol{I}(\boldsymbol{p}) > \boldsymbol{I}(\alpha \boldsymbol{p})$

Given a standard interference function $\boldsymbol{I}(\boldsymbol{p})$, the iteration (9) was defined as the *standard* power control algorithm. When $\boldsymbol{p} \ge \boldsymbol{I}(\boldsymbol{p})$, we say that $\boldsymbol{p}$ is a feasible power vector. In [12], the following claim was verified.

Theorem 1: If there exists a power vector $\boldsymbol{p}'$ satisfying $\boldsymbol{p}' \ge \boldsymbol{I}(\boldsymbol{p}')$, then starting from any initial power vector $\boldsymbol{p}$, the standard power control iteration converges to a unique fixed point $\boldsymbol{p}^*$ such that $\boldsymbol{p}^* \le \boldsymbol{p}'$ for any feasible power vector $\boldsymbol{p}'$.

We will also need results regarding the componentwise minimum and maximum of two interference functions. Specifically, given two standard interference functions $\boldsymbol{I}(\boldsymbol{p})$ and $\boldsymbol{I}'(\boldsymbol{p})$, we define $\boldsymbol{I}^{\max}(\boldsymbol{p})$ and $\boldsymbol{I}^{\min}(\boldsymbol{p})$ by

$$\begin{aligned} \boldsymbol{I}_j^{\max}(\boldsymbol{p}) &= \max\left\{\boldsymbol{I}_j(\boldsymbol{p}), \boldsymbol{I}'_j(\boldsymbol{p})\right\} \\ \boldsymbol{I}_j^{\min}(\boldsymbol{p}) &= \min\left\{\boldsymbol{I}_j(\boldsymbol{p}), \boldsymbol{I}'_j(\boldsymbol{p})\right\} \end{aligned}$$

The following claim is readily verified.

Theorem 2: If $\boldsymbol{I}(\boldsymbol{p})$ and $\boldsymbol{I}'(\boldsymbol{p})$ are monotone and scalable, then $\boldsymbol{I}^{\min}(\boldsymbol{p})$ and $\boldsymbol{I}^{\max}(\boldsymbol{p})$ are monotone and scalable.

Note that when $\boldsymbol{I}(\boldsymbol{p}) = \boldsymbol{r}$ where $\boldsymbol{r}$ is a positive constant vector, it is trivially true that $\boldsymbol{I}(\boldsymbol{p})$ is a standard interference function. Thus, Theorem 2 has the following corollary,

Corollary 1: For positive power vectors $\boldsymbol{p}^{\min}$ and $\boldsymbol{p}^{\max}$ and a scalable and monotone interference function $\boldsymbol{I}(\boldsymbol{p})$, $\boldsymbol{I}''(\boldsymbol{p})$ defined by

$$I''_j(\boldsymbol{p}) = \max\left(p_j^{\min}, \min\left(p_j^{\max}, I_j(\boldsymbol{p})\right)\right)$$

is a standard interference function. Since $\boldsymbol{p}^{\max} \ge \boldsymbol{I}''(\boldsymbol{p}^{\max})$, the iteration $\boldsymbol{p}(t+1) = \boldsymbol{I}''(\boldsymbol{p}(t))$ always converges to a unique fixed point.

The consequence of Corollary 1 is that if $\boldsymbol{T}(\boldsymbol{p})$ from (6) meets the requirements of a standard interference function, the iteration (8) is guaranteed to converge.

IV. Soft Dropping Convergence

In this section, we analyze the synchronous constrained power control iteration (8) in which users repeatedly adjust their transmitter powers to meet the variable target SIR constraints (3). From Figure 1, the variable target SIR $\Gamma_j(p_j)$ can be written

$$\Gamma_j(p_j) = \begin{cases} \overline{\Gamma}_j & p_j \le \bar{q}_j \\ \Gamma_j^{(v)}(p_j) & \bar{q}_j < p_j < \hat{q}_j \\ \hat{\Gamma}_j & p_j \ge \hat{q}_j \end{cases} \tag{10}$$

From (6) and (10), we can write

$$T_j(\boldsymbol{p}) = \begin{cases} \overline{T}_j(\boldsymbol{p}) & p_j \le \bar{q}_j \\ T_j^{(v)}(\boldsymbol{p}) & \bar{q}_j < p_j < \hat{q}_j \\ \hat{T}_j(\boldsymbol{p}) & p_j \ge \hat{q}_j \end{cases} \tag{11}$$

From (1) and (6), we observe that

$$\overline{T}_j(\boldsymbol{p}) = \overline{\Gamma}^{\beta_j} p_j^{1-\beta_j} I_j^{\beta_j}(\boldsymbol{p}) \tag{12}$$

$$\hat{T}_j(\boldsymbol{p}) = \hat{\Gamma}^{\beta_j} p_j^{1-\beta_j} I_j^{\beta_j}(\boldsymbol{p}) \tag{13}$$

To identify $\boldsymbol{T}^{(v)}(\boldsymbol{p})$, we observe from Figure 1 that the slope of $\Gamma_j^{(v)}(p_j)$ equals $-\delta_j$ where

$$\delta_j = \frac{\log(\overline{\Gamma}_j/\hat{\Gamma}_j)}{\log(\hat{q}_j/\bar{q}_j)} \tag{14}$$

From (6), (11) and (14), it can be verified that

$$T_j^{(v)}(\boldsymbol{p}) = \overline{\Gamma}_j^{\beta_j}\,\bar{q}_j^{\beta_j\delta_j}\,p_j^{1-\beta_j(1+\delta_j)}\,I_j^{\beta_j}(\boldsymbol{p}) \tag{15}$$

To prove convergence of the iteration (8), we will need the following lemma.

Lemma 1: If $\boldsymbol{I}(\boldsymbol{p})$ is standard, then $\boldsymbol{I}'(\boldsymbol{p})$ defined by $I_j'(\boldsymbol{p}) = c_j p_j^{\mu_j} I_j^{\beta_j}(\boldsymbol{p})$ is scalable and monotone if for all j, $c_j > 0$, $\beta_j > 0$, $\mu_j \geq 0$, and $\mu_j + \beta_j \leq 1$.

From Lemma 1, we have the following corollary.

Theorem 3: If $0 \leq \beta_j \leq (1+\delta_j)^{-1}$ for all j, the interference functions $\hat{\boldsymbol{T}}(\boldsymbol{p})$, $\boldsymbol{T}^{(v)}(\boldsymbol{p})$ and $\overline{\boldsymbol{T}}(\boldsymbol{p})$ are all scalable and monotone.

Further, we observe that

$$T_j^{(v)}(\boldsymbol{p}) \leq \overline{T}_j(\boldsymbol{p}) \quad \text{iff} \quad p_j \geq \bar{q}_j \tag{16}$$

$$T_j^{(v)}(\boldsymbol{p}) \leq \hat{T}_j(\boldsymbol{p}) \quad \text{iff} \quad p_j \geq \hat{q}_j \tag{17}$$

From (11), this implies that the iteration function $\boldsymbol{T}(\boldsymbol{p})$ can be written as

$$T_j(\boldsymbol{p}) = \max[\hat{T}_j(\boldsymbol{p}), \min[\overline{T}_j(\boldsymbol{p}), T_j^{(v)}(\boldsymbol{p})]] \tag{18}$$

By Theorem 2, we see that $\boldsymbol{T}'(\boldsymbol{p})$ defined by $T_j'(\boldsymbol{p}) = \min[\overline{T}_j(\boldsymbol{p}), T_j^{(v)}(\boldsymbol{p})]$ is scalable and monotone and thus $T_j(\boldsymbol{p}) = \max[\hat{T}_j(\boldsymbol{p}), T_j'(\boldsymbol{p})]$ is also scalable and monotone. This result implies the following corollary.

Corollary 2: The constrained iteration function $\boldsymbol{T}^*(\boldsymbol{p})$ defined by (7) is a standard interference function.

Thus, the power constrained iteration (8) always converges to a unique fixed point at which each user transmits with the minimum possible transmitted power subject to variable target SIR requirements and minimum and maximum power constraints.

V. Simulation Model

The convergence analysis of Section I is valid for a single channel system. In this section, we will study the performance of an asynchronous, distributed Soft Dropping Power Control algorithm in a channelized system by simulation of a two dimensional macro-cellular system. Base station assignment and dynamic channel allocation scheme alongwith Received signal strength index (RSSI) based handoff schemes and least interference dynamic channel allocation algorithms are also simulated. To assess the performance improvement of soft dropping, we compare with the ordinary fixed target power control algorithm.

For a two dimensional macro cellular system, we assume a Manhattan-like road grid which is formed into a torus-like structure to avoid edge effects. B = 48 base stations (BS) are spaced uniformly 2000 m apart vertically and 1500m horizontally; see Figure 2. A nominal hexagonal cell geometry can be assumed depending on the path gain. A common set of M = 30 channels are available at each base station.

A mobile's speed follows a truncated Gaussian distribution with mean speed of 90 km/hr and standard deviation of 15 km/hr, truncated at a minimum speed of 60 km/hr and maximum speed of 120km/hr. The new call arrivals are uniformly distributed over all roads and the two directions along the road are equally likely. Traffic is allowed only along the grid lines, to avoid complexity. Free flowing highway traffic is assumed, in other words each mobile moves along the road unaware of any other mobile on the same path. The velocity of the mobile remains fixed throughout the duration of a call.

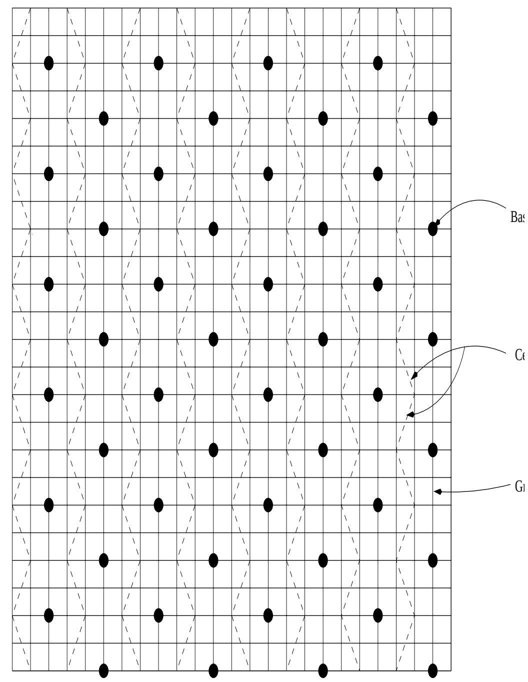

Fig. 2. Two-dimensional macro-cell environment

The new call arrival process is an independent Poisson process with mean arrival rate λ calls per second. Call durations are independent exponential random variables with mean $1/\mu$=120 sec. With B base stations, the normalized traffic load is $\rho = \lambda/(\mu\text{MB})$ erlangs/cell/channel. The radio link gain includes both a propagation loss model of order α = 4 and shadow fading. That is, the link gain h_{kj} from the user j at a distance d_{kj} to base k in units of dB is

$$10\log h_{kj} = -10\alpha\log d_{kj} + S_j(d_{kj}) \tag{19}$$

where $S_j(d_{kj})$, the position dependent shadow fading factor, is modeled as a zero mean Gaussian random variable with standard deviation σ=6 dB. The shadow fading at each base station is modeled as an independent spatial process with exponential autocorrelation

$$R_{S_j}(\Delta d_{kj}) = \sigma^2 e^{-\Delta d/D} \tag{20}$$

We assume that every base station transmits a pilot tone at a constant power level. The new user listens to all the bases and is assigned to the base with the strongest received pilot. At that base, the new user is assigned to the channel with the least interference. We consider an admission control based on SIR threshold, Γ_{new}, as described in [16]. A new call is accepted only if the assigned channel h can provide an estimated minimum SIR that is not less than Γ_{new}.

If a terminal finds that the RSSI (path gain) of a neighboring base station is hys higher than that the user is presently connected to, it will attempt an intercell handoff to that base station. An intercell handoff attempt fails if the base station is unable to find an unoccupied channel or it does not have sufficient power to achieve the target SIR on the allocated channel. The call is dropped if the SIR remains below the threshold for longer than the outage duration t_{out} whether it is able to perform an intercell handoff or not.

Although the theoretical properties of a the soft dropping algorithm appear desirable, a practical implementation is of prime importance. Thus we have attempted to simulate the power control iteration in a GSM environment for Class 5 mobile stations. In other words, the transmitter power of every user is asynchronously changed by 2 dB at a rate of 10 iterations/sec depending on the current quality of its connection. Further, each user is subject to minimum and maximum power constraints.

The two set of limits, each for target SIR and uplink power for soft dropping are crucial to the performance of the system. The soft dropping upper limit SIR is $\overline{\Gamma}_j = 20$ dB and the lower limit is $\hat{\Gamma}_j = 17$ dB. For the fixed target algorithm, the target is set at 20 dB. In all cases, the dropping threshold is set at $\Gamma_d = 16$ dB. Other simulation parameters are summarized in Table I.

h	Height of antenna	50 m
M	No. of channels in each cell	30
D	Shadow Fading correlation dist.	50 m
N_0	Receiver Noise Power	-150 dBm
$p^{\max}$	Maximum transmitter power	0.8 W
$p^{\min}$	Minimum transmitter power	19.9 mW
t_{out}	Outage duration	5 sec
Γ_{new}	New call SIR threshold	21 dB
$\hat{q}_j$	Soft dropping upper power limit	-1 dB

TABLE I

OTHER SIMULATION PARAMETERS

VI. RESULTS AND ANALYSIS

The system performance is measured in terms of the following parameters

$$P_b = \text{new calls blocked/call arrivals} \tag{21}$$

$$P_d = \text{dropped calls/accepted calls} \tag{22}$$

Since dropping an existing call is believed to be more detrimental than blocking a new call, we have also considered a weighted service denial rate $P_b + 10P_d$. We will also examine the mean uplink transmitter power level as another figure of merit.

Figures 3 and 4 examine the impact RSSI hysteresis for soft dropping with $\overline{q}_j = -15$ dB. Consistent with [16], it is found that a small RSSI leads to more handoffs back and forth between two adjacent bases while large hysteresis delays

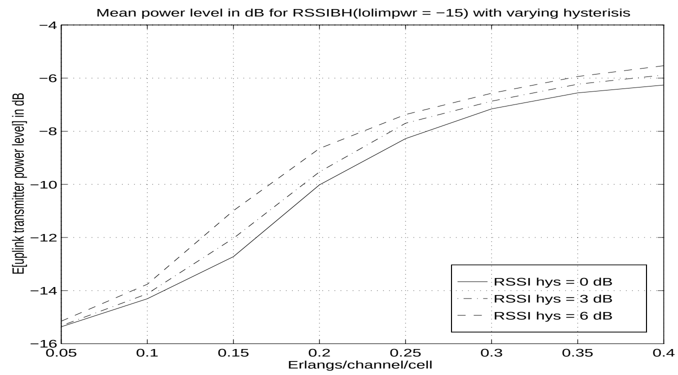

Fig. 3. Avg. power level in dB (Hys = 0, 3, 6 dB)

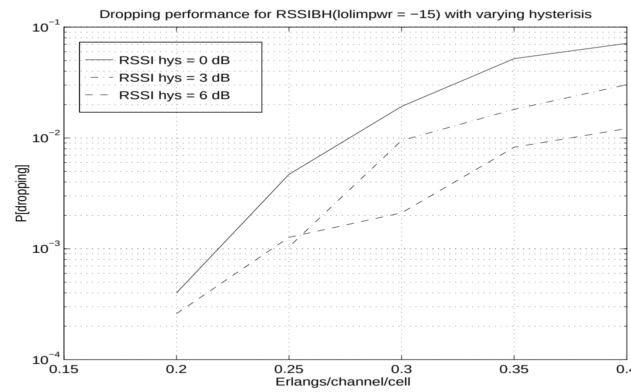

Fig. 4. P_d vs. traffic (hys $= 0, 3, 6$ dB)

the handoff until the mobile is relatively close to the new base. hence, when an MS employing large hysteresis attempts a handover, it is more likely to succeed. However, larger hysteresis causes power levels to be higher than necessary. These effects can be observed in Figure 4 which shows the reduction in dropped calls and Figure 3 which displays the increase in the average power level with increase in RSSI hysteresis.

Figures 5 through 7 compare the soft dropping algorithm with a varying lower limit ($\overline{q}_j$= -5 dB, -11 dB, -15 dB) on transmitted power. to the fixed target scheme. In Figure 5, We can clearly observe the improvement in power consumption when compared to a fixed target. We observe there exists a trade-off in the selection of the lower limit on power $\overline{q}_j$. Reducing $\overline{q}_j$ leads to a considerable reduction in the transmitter power levels; however, it is also responsible for overall deterioration in call quality The decrease in power levels can be attributed to the fact that fewer users will aim for the upper limit SIR $\overline{\Gamma}_j$. This tends to reduce the level of co-channel interference in the system. The result is that a relatively more calls are admitted to the system (Figure 6) but fewer calls are dropped (Figure 7).

We have seen that soft dropping can provide noticeable prformance improvements even in a GSM environment where the power control is relatively slow and coarse. The general approach of soft dropping can be applied to almost any power

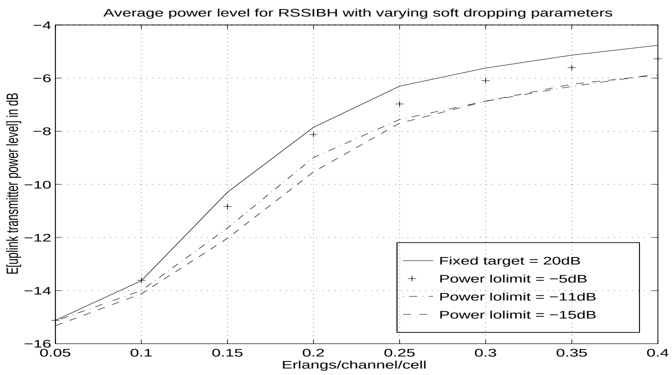

Fig. 5. Avg. power level in dB with lower limit $\overline{q}_j = -5, -11, -15$ dB)

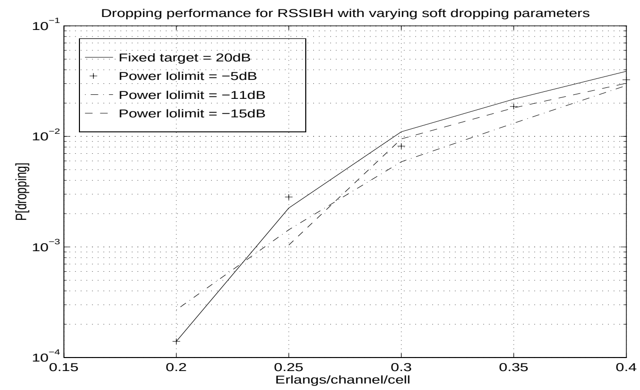

Fig. 7. P_d vs. traffic ($\overline{q}_j$= -5, -11, -15 dB)

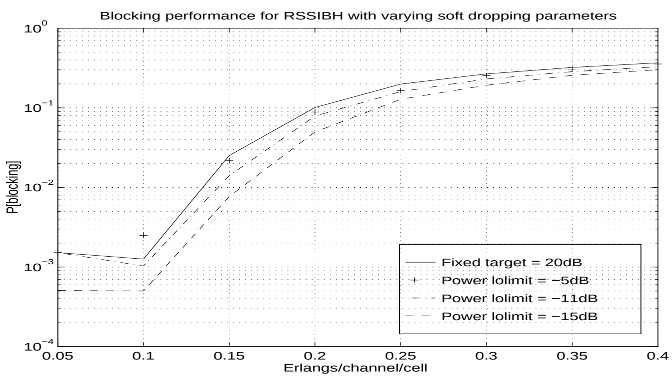

Fig. 6. P_b vs. traffic ($\overline{q}_j$= -5, -11, -15 dB)

controlled system. We expect that in other environments, notably IS-95, the improvements may be even more dramatic.

REFERENCES

[1] J. M. Aein. Power balancing in system employing frequency reuse. *COMSAT Technical Review*, 3(2), Fall 1973.

[2] H. J. Meyerhoff. Method for computing the optimum power balancing in multibeam satellite. *COMSAT Technical Review*, 4(1), Spring 1974.

[3] R.W. Nettleton and H. Alavi. Power control for spread-spectrum cellular mobile radio system. In *Proc. IEEE Vehicular Technology Conference, VTC'83*, 1983.

[4] W. Tschirks. Effects of transmission power control on the cochannel interference in cellular radio networks. *Electrotechnik und Informationstechnik*, 106(5), 1989.

[5] S. Grandhi, R. Vijayan, D. J. Goodman, and J. Zander. Centralized power control for cellular radio systems. *IEEE Transactions on Vehicular Technology*, 42(4), November 1993.

[6] J. Zander. Performance of optimum transmitter power control in cellular radio systems. *IEEE Transactions on Vehicular Technology*, 41, February 1992.

[7] G.J. G.J. Foschini and Z. Miljanic. A simple distributed autonomous power control algorithm and its convergence. *IEEE Transactions on Vehicular Technology*, 42(4), November 1993.

[8] D. Mitra. An asynchronous distributed algorithm for power control in cellular radio systems. In *Fourth WINLAB Workshop on Third Generation Wireless Information Networks*, 1993.

[9] S. V. Hanly. An algorithm for combined cell-site selection and power control to maximize cellular spread spectrum capacity. *IEEE Journal on Selected Areas in Communications*, 13(7):1332–1340, September 1995.

[10] R. Yates and C.Y. Huang. Integrated power control and base station assignment. *IEEE Transactions on Vehicular Technology*, 44(3), August 1995.

[11] R. Yates and C.Y. Huang. Constrained power control and base station assignment in cellular radio systems. *IEEE/ACM Transactions on Networking*, 1995. (in press).

[12] R. Yates. A framework for uplink power control in cellular radio systems. *IEEE J. Sel. Areas Commun.*, 13(7):1341–1348, September 1995.

[13] S. Grandhi and J. Zander. Constrained power control in cellular radio systems. In *Proc. IEEE Vehicular Technology Conference, VTC-94*, 1994.

[14] S.A. Grandhi. *Power Control in Mobile Radio Systems*. PhD thesis, Rutgers University, 1994.

[15] M. Almgren, H. Andersson, and K. Wallstedt. Power control in a cellular system. In *IEEE Vehicular Technology Conference VTC-94*, pages 833–837, 1994.

[16] C.N. Chuah, R. Yates, and D. Goodman. Integrated dynamic radio resource managemant. In *Proc. IEEE Vehicular Technology Conference, VTC-95*, pages 584–588, 1995.